



HAL
open science

DNA polymerization in icy moon abyssal pressure conditions

Lorenzo Carré, Ghislaine Henneke, Etienne Henry, Didier Flament, Éric Girard, Franzetti Bruno, Bruno Franzetti

► **To cite this version:**

Lorenzo Carré, Ghislaine Henneke, Etienne Henry, Didier Flament, Éric Girard, et al.. DNA polymerization in icy moon abyssal pressure conditions. *Astrobiology*, 2023, pp.0201. 10.1089/ast.2021.0201 . hal-03944643

HAL Id: hal-03944643

<https://hal.science/hal-03944643>

Submitted on 24 Nov 2023

HAL is a multi-disciplinary open access archive for the deposit and dissemination of scientific research documents, whether they are published or not. The documents may come from teaching and research institutions in France or abroad, or from public or private research centers.

L'archive ouverte pluridisciplinaire **HAL**, est destinée au dépôt et à la diffusion de documents scientifiques de niveau recherche, publiés ou non, émanant des établissements d'enseignement et de recherche français ou étrangers, des laboratoires publics ou privés.

DNA Polymerization in Icy Moon Abyssal Pressure Conditions

Carré Lorenzo ¹, Henneke Ghislaine ², Henry Etienne ³, Flament Didier ², Girard Éric ¹, Franzetti Bruno ^{1,*}

¹ University of Grenoble Alpes, CNRS, CEA, IBS, Grenoble, France.

² Laboratoire de Microbiologie des Environnements Extrêmes, CNRS, Ifremer, Université de Brest, Plouzané, France.

³ Laboratoire de Microbiologie des Environnements Extrêmes, CNRS, Ifremer, Université de Brest, Plouzané, France.

* Corresponding author : Bruno Franzetti, email address : franzetti@ibs.fr

Abstract :

Evidence of stable liquid water oceans beneath the ice crust of moons within the Solar System is of great interest for astrobiology. In particular, subglacial oceans may present hydrothermal processes in their abysses, similarly to terrestrial hydrothermal vents. Therefore, terrestrial extremophilic deep life can be considered a model for putative icy moon extraterrestrial life. However, the comparison between putative extraterrestrial abysses and their terrestrial counterparts suffers from a potentially determinant difference. Indeed, some icy moons oceans may be so deep that the hydrostatic pressure would exceed the maximal pressure at which hydrothermal vent organisms have been isolated. While terrestrial microorganisms that are able to survive in such conditions are known, the effect of high pressure on fundamental biochemical processes is still unclear. In this study, the effects of high hydrostatic pressure on DNA synthesis catalyzed by DNA polymerases are investigated for the first time. The effect on both strand displacement and primer extension activities is measured, and pressure tolerance is compared between enzymes of various thermophilic organisms isolated at different depths.

32 Introduction

33

34 Terrestrial life is possible under a large range of chemical and physical
35 conditions. Extremophilic microorganisms push the boundaries of these ranges further than
36 what can be expected from an anthropocentric point of view, inhabiting extreme
37 environments which were previously thought to be too hostile for life. Yet, even extremophilic
38 life is limited to environments above a certain level of water availability (Hallsworth *et al.*,
39 2007; Belilla *et al.*, 2019). Hence, looking for liquid water bodies remains essential for the
40 search of extraterrestrial life and habitable environments. In this context, the subglacial
41 oceans of icy moons of the Solar System are of particular interest (Jebbar *et al.*, 2020; Taubner
42 *et al.*, 2020). Among them, Europa and Enceladus retain most of the attention. Several lines
43 of evidence show that the water would be in interaction with rock, enabling enrichment of
44 subglacial ocean with various ions, metals and organic molecules. Characterization of these
45 interactions is indeed a major goal of future space missions (Pappalardo, 2012; Cable *et al.*,
46 2016). Moreover, these subglacial oceans may possess hydrothermal processes at their
47 bottom. While stronger evidence support this hypothesis for Enceladus (Matson *et al.*, 2007;
48 Hsu *et al.*, 2015; Sekine *et al.*, 2015; Waite *et al.*, 2017), geochemical models also argue in
49 favor of abyssal hydrothermal processes for Europa (Lowell and DuBose, 2005; Zolotov, 2007).

50 Such extraterrestrial abyssal hydrothermal environments would be expected to show
51 similarities with their terrestrial counterparts: hydrothermal vents and black smokers. On
52 Earth, these oceanic environments are observed at various depths, ranging from shallow
53 waters to 5km deep. While displaying extreme conditions such as temperature, pressure and
54 sometimes alkaline pH or heavy metal abundancy, these environments are actually associated
55 with complex and diverse ecosystems, offering energy sources and chemical and physical
56 gradients for life. In the absence of light, the primary producers of hydrothermal vent
57 environments are extremophilic chemolithotrophs. These microorganisms, either belonging
58 to the *Bacteria* or *Archaea* domain, therefore make good models for testing habitability and
59 have already been used as such (Taubner *et al.*, 2018).

60 However, the physical and chemical conditions may differ in extraterrestrial abysses.
61 On Earth, deepest hydrothermal vent lies at approximatively 5km under the sea level with *in*
62 *situ* pressure of 50MPa (Connelly *et al.*, 2012) and deepest point in the ocean is met in the
63 Mariana Trench at 11km under the sea level at a pressure of approximatively 108MPa. In shear
64 contrast, subglacial oceans of several moons could be hundreds kilometers deep (Schmidt and
65 Manning, 2017). On Europa for example, the ocean is expected to be, depending on the
66 model, up to 100-200km deep (Anderson *et al.*, 1997, 1998; Pappalardo *et al.*, 1999; Spohn
67 and Schubert, 2003; Marion *et al.*, 2003; Thomas *et al.*, 2016) and beneath a 10km thick ice
68 shell (Park *et al.*, 2015), reaching hydrostatic pressures as high as 130-260MPa (Naganuma
69 and Uematsu, 1998).

70 Even though most of the terrestrial biosphere is permanently under high hydrostatic
71 pressure (HHP), as 88% of the ocean volume is above 10MPa (Jebbar *et al.*, 2015), its effects
72 on complex biological processes remains to be explored. Deep sea organisms have to cope
73 with effects of HHP at the molecular level. Indeed, following Le Chatelier's principle, increases
74 of HHP promotes reduction of volume through production of charges and condensation of
75 biomolecules (Gross and Jaenicke, 1994; Abe *et al.*, 1999). In particular, dissociation of large

76 molecular assemblies such as ribosomes (Gross *et al.*, 1993) and DNA-protein complexes
77 (Kawano *et al.*, 2005) is favored under HHP. Upon higher pressure increase, protein unfolding
78 is facilitated (Jebbar *et al.*, 2020), most proteins losing their tertiary structure at 400MPa
79 (Aertsen *et al.*, 2009). Before unfolding, HHP may have either an inhibitory or a stimulating
80 effect on enzymatic activity, depending on the enzyme (Eisenmenger and Reyes-De-Corcuera,
81 2009). Notably, a peptidase complex from an abyssal hyperthermophilic *Archaea* have
82 showed to be activated by HHP (Rosenbaum *et al.*, 2012). DNA is also reversibly compacted
83 by HHP but remains exceptionally stable as it resists denaturation at even 1GPa (Hedén *et al.*,
84 1964; Girard *et al.*, 2007). Experimental data actually show that nucleic acids are stabilized by
85 high hydrostatic pressure (Macgregor, 1996; Dubins *et al.*, 2001). As a consequence, all
86 biological processes requiring an opening of the DNA double-helix, such as replication,
87 transcription and translation, can be impaired by high hydrostatic pressure (Macgregor, 2002).

88 Yet, DNA synthesis has never been studied under HHP. DNA replication is one of the
89 most conserved process, which must occur in every cell before cell division, thus, to ensure
90 successful inheritance of genetic traits. *In cellulo* this process is catalyzed by a class of enzymes
91 called DNA polymerases (DNAPs) which take part of a larger complex, the replisome. DNAPs
92 require a DNA strand primed by a DNA or RNA strand with 3'-hydroxyl extremity,
93 deoxyribonucleotide triphosphates (dNTPs) and divalent cations, Mg²⁺ or Ca²⁺ (Ralec *et al.*,
94 2017). The simplicity of this process has made possible all existing PCR technologies, allowing
95 fast and unexpensive amplification of DNA. In this context, thermostable DNAPs from
96 organisms isolated in hot environments are routinely used. In particular, many B-family DNA
97 polymerases from hyperthermophilic *Archaea*, showing high thermostability, extension rate
98 and fidelity have been characterized (Zhang *et al.*, 2015). Some were isolated from deep sea
99 organisms which are permanently exposed to high hydrostatic pressure. While their activity is
100 high at ambient pressure, there has been no characterization at physiological or even higher
101 pressure conditions. To our knowledge, it has only been showed that a pressure of 89MPa
102 strongly enhances thermostability of DNA polymerases from both deep sea and shallow
103 waters (Summit *et al.*, 1998).

104 In this study, effects of HHP as high as 100MPa on activity of five thermostable DNAPs
105 are investigated for the first time.

106 Material and methods

107

108 DNAPs production and purification

109

110 To facilitate interpretation of the effects of HHP on polymerase activity, we only used
111 enzymes without 3' → 5' exonuclease activity, which allows proofreading, either naturally
112 deprived of this activity or by using exonuclease-deficient mutants (*exo*⁻).

113 Exonuclease-deficient *Pyrococcus abyssi* B-family DNAP (*PabPolB* *exo*⁻) (D215A) with a
114 Nter his-tag sequence MGSSHHHHHSSGLVPRGSH was produced and purified as previously
115 described (Gueguen *et al.*, 2001; Gouge *et al.*, 2012). Briefly, enzyme was recombinantly
116 expressed in *Escherichia coli* Rosetta 2 (DE3) cells transformed with a pET28 vector (Novagen)
117 in which gene of *PabPolB* *exo*⁻ was inserted between NdeI and BamHI restriction sites. Cells
118 were grown to an optical density of 0.7 in LB medium at 37°C under shaking and in presence
119 of kanamycine (50mg.mL⁻¹). Expression was then induced by addition of 1mM IPTG and cells
120 were incubated overnight at 30°C. After centrifugation at 3000g for 20min at 4°C, cell pellets
121 were suspended in 50mM Tris/HCl pH 7, 200mM NaCl, 9mM imidazole and 0.1% triton X-100
122 buffer to which were added protease inhibitors (Roche). Cells were lysed by sonication and
123 lysate was incubated 1h at ambient temperature after addition of 50µg.mL⁻¹ of DNase I. A heat
124 treatment of 75°C during 30min was applied to the supernatant before purifying the protein
125 by column chromatography. HisTrapHP™ with nickel-affinity resin, HiTrap™ Heparin HP with
126 affinity for DNA-binding proteins and size exclusion Superdex™ 200 10/300 GL columns (GE
127 Healthcare) were successively used. After dialysis, protein was stored at -20°C in a final buffer
128 containing 50mM Tris-HCl, pH7.5, and 2mM MgCl₂. Quality and purity of sample was checked
129 by electrospray ionization (ESI) at the mass spectrometry platform at IBS. Observed mass of
130 dominant species was in agreement with a loss of MGSSHHH at Nter. A final concentration of
131 1.16µM (0.106mg/mL) of protein was measured with a NanoDrop™ device from
132 ThermoFisher. Molar extinction coefficient was determined using an online calculator
133 (<https://web.expasy.org/cgi-bin/protparam/protparam>).

134 Other proofreading-lacking DNAPs were all purchased. *Taq* from *Thermus aquaticus*,
135 Vent® (*Tli*) *exo*⁻ from *Thermococcus littoralis*, and Deep Vent® (*Psb*) *exo*⁻ from
136 *Pyrococcus* specie GB-D were purchased from New England Biolabs. *Pfu* *exo*⁻ from *Pyrococcus*
137 *furiosus* was obtained from Agilent. Concentrations of purchased polymerases were given by
138 the manufacturers and were all equal to 2000units.mL⁻¹.

139

140 Oligonucleotides and template DNA

141 For extension assays, template DNA was the M13mp18 singled-stranded circular DNA,
142 7249 nucleotides (nt) in length, purchased from New England Biolabs. For experiments at
143 55.5-65.0°C, the template was primed with a 30nt primer whose sequence was
144 TGCCAAGCTTGCATGCCTGCAGGTCGACTC. For gel analysis experiments, this primer was
145 labelled at the 5' end with a Cy5 fluorophore. Since primer-template interaction was no longer
146 stable at higher temperatures, we used an 87nt primer instead whose sequence was
147 TGCCAAGCTTGCATGCCTGCAGGTCGACTCTAGAGGATCCCCGGTACCGAGCTCGAATTCGTAATC
148 ATGGTCATAGCTGTTTCCTG for experiments at 70.0°C.

149 For strand displacement assays, template DNA was an oligonucleotide 87nt in length
150 whose sequence was
151 CAGGAAACAGCTATGACCATGATTACGAATTCGAGCTCGGTACCCGGGGATCCTCTAGAGTCGACCT
152 GCAGGCATGCAAGCTTGGCA and which was labelled with a 6-FAM fluorophore at the 5'-end
153 and primed with a 30nt quencher whose sequence was
154 TGCCAAGCTTGCATGCCTGCAGGTCGACTC. Fluorescence was initially quenched by a Deep Dark
155 Quencher I 3'-modification harbored by a 30nt oligonucleotide, whose sequence was
156 ATTCGTAATCATGGTCATAGCTGTTTCCTG, complementary to the sequence of the template
157 from the 5'-end.

158 All oligonucleotides were purchased from Eurogentec (Seraing, Belgium).

159

160 High-pressure real-time fluorimetry

161 All fluorescence measurements were performed at various temperatures using a Jasco
162 (Tokyo, Japan) FP-750 spectrofluorometer modified to accommodate a high-pressure cell
163 manufactured by Top Industrie (Vaux-le-Pénil, France). 200µL of reaction mixtures were
164 prepared to be put in custom rectangular quartz microcuvettes manufactured by Jasco (Tokyo,
165 Japan) which were sealed with plastic film and joint as follows: approx 1cm² of plastic film was
166 placed on top of the microcuvette and an O-ring joint from Sephat (Palaiseau, France) was
167 placed over it to maintain the seal. Mixture volume slightly exceeded microcuvette volume to
168 prevent the entrapment of an air bubble. No evidence of sample leak could be observed with
169 experiments and controls. In particular, no sign of mechanical constraint on plastic film or O-
170 ring joint was seen. Excessive reaction mixture was removed prior to the experiment.

171 The measurement chamber was filled with distilled water at the desired temperature.
172 The microcuvette was inserted in a custom metal adapter, which allows fluorescence
173 measurement, then put inside the high-pressure cell while immediately starting signal
174 acquisition. To prevent entrapment of an air bubble inside, excessive water was present in the
175 chamber and removed during closure of the chamber. This allowed a better control and
176 monitoring of temperature equilibrium of the sample.

177 After sealing, pressure was increased with a manual pump linked to the high-pressure
178 cell through a water-filled metal capillary tube connected to the chamber. Pressure was
179 monitored with a probe manufactured by Top Industrie (Vaux-le-Pénil, France), located
180 between pump and high-pressure cell. HHP were typically reached in 1-2min.

181 Temperature inside the chamber was controlled through the circulation of a heat
182 transfer fluid made with tap water supplemented with 30% ethylene glycol and anti-algae
183 Aqua Stabil from Julabo (Seelbach, Germany). This fluid circulated within the high-pressure
184 cell separately from the chamber and the capillary and was heated with a CORIO CD-200F
185 refrigerated/heating circulator purchased from Julabo (Seelbach, Germany). The temperature
186 to which the circulator had to be set to reach the desired temperature for the reaction was
187 empirically determined by measuring it in the chamber under ambient pressure with a
188 calibrated thermocouple.

189

190 Real-time strand displacement assays

191 For real-time strand displacement assays, we used a modified tripartite DNA hybrid
192 (Dorjsuren *et al.*, 2009). Reaction mixtures consisted of 50mM Tris-HCl pH8.8, 50mM KCl, 2mM

193 MgCl₂, 2mM DTT, 200μM dNTPs, 200nM tripartite DNA hybrid. *PabPolB* *exo*⁻ enzyme
194 concentration was 46,4nM.

195 Excitation was made continuously at 480nm and emission at 525nm was measured
196 every second. Total run length was 15min.

197

198 Real-time extension assays

199 For real-time extension assays, reaction mixtures consisted of 50mM Tris-Hcl pH8.8,
200 50mM KCl, 2mM MgCl₂, 2mM DTT, 200μM dNTPs, 418pM primed M13mp18. Picogreen™
201 (Thermofisher) was added at final 3200-fold dilution from the commercial solution. All
202 commercial enzymes were incubated in the same buffer, except *Pfu* *exo*⁻ which was incubated in
203 the buffer provided by the manufacturer (Agilent). *PabPolB* *exo*⁻ enzyme concentration was 46.4
204 nM. Commercial enzymes were used at a concentration of 0.01 unit.mL⁻¹.

205 Excitation was made at 485nm every 20s and emission at 520nm was measured for 1s.
206 Total run length was either 15 or 30min.

207

208 Gel analysis of products

209 Reactions were conducted similarly to the real-time extension assays in the same
210 thermostated fluorescence cell with the fluorimeter turned off and without picogreen. The
211 primer was labelled with a Cy5 fluorophore at the 5' end. After a 30min extension reaction
212 under various pressures, decompression, chamber opening and sample retrieval were
213 performed as fast as possible and reactions were stopped by adding an equal volume of 95%
214 formamide, 10mM EDTA on ice. This procedure took approximatively 60s, from the start of
215 decompression to the addition of the formamide. Primer extension products (20 μL) were
216 loaded onto TAE-agarose 1% gels and separated by electrophoresis at 100V and 100mA for 5
217 h. Bands containing hybridized extended Cy5-labelled primer were revealed with a Gel Doc
218 XR+ Gel Documentation System (Bio-Rad) used with the fluorescence mode.

219 Results

220

221 Gel analysis of products synthesized under HHP

222

223 We first determined effects of HHP on global DNA synthesis by *PabPolB* exo^- by
224 analyzing, after decompression of the sample, the length of primer extension products
225 synthesized under various pressure values and at 55.5 or 65.0°C. Fluorescent products labelled
226 with Cy5 at the 5' end of the elongated 30nt primer were separated on agarose gel
227 electrophoresis (Figure 1).

228 Products were longer at 65.0°C than at 55.5°C. In contrast, gradual decrease of product
229 length as pressure increased was observed, from 50MPa at 55.5°C and from 25MPa at 65.0°C.
230 Little or no increase in product length in comparison with the negative control were observed
231 at 100MPa in both conditions.

232

233 Real-time monitoring of strand displacement activity under HHP

234

235 To analyze effects of HHP in real-time, we used a fluorescence-based tripartite
236 oligonucleotide template system relying on strand-displacement activity by B-family DNAPs
237 (Canceill *et al.*, 1999; Henneke, 2012). The increase of fluorescence caused by strand
238 displacement of the oligonucleotide quenching the fluorescent signal of 87nt template was
239 used as proxy for *PabPolB* activity. Strand displacement assays were performed for 30min at
240 55.5°C under 0.1, 10, 50 and 100MPa three times independently (Figure 2).

241 Fluorescence signal of positive control (6-FAM labelled template annealed to extension
242 primer without the quenching oligonucleotide) slightly decreased over time, presumably
243 caused by photobleaching of the 6-FAM fluorophore. Pressure gradually delayed and slowed
244 down the increase of fluorescence in the enzymatic assays, showing an inhibiting effect on
245 strand displacement activity. The inhibition could be observed from 10MPa and little or no
246 activity could be observed at 100MPa.

247 These experiments were also conducted at additional temperature (55.5, 60, 65,
248 70.0°C) and pressure values (0.1, 35, 50 and 100MPa) (Supplementary Figure 1). Fluorescence
249 increase was faster at 60 and 65.0°C than at 55.5°C. In contrast, at every temperature, HHP
250 gradually delayed fluorescence increase. Fluorescence curve of the unquenched template was
251 slightly higher at 65.0°C than at 55.5 and 60.0°C, which may indicate that basal signal of the
252 fluorophores is dependent on the temperature. At temperatures above theoretical melting
253 temperatures (T_m) of primer in the presence of the quenching oligonucleotide, respectively
254 58.9°C and 67.1°C, spontaneous denaturation of the tripartite DNA may however have
255 happened, as showed by the increase of fluorescence of the negative control at 70.0°C.

256

257 Real-time monitoring of primer extension activity under HHP

258

259 Primer extension activity was also directly monitored by measuring the fluorescence
260 of picogreen which increases as it intercalates in increasing amounts of double-stranded DNA
261 during primer extension. The DNA template was single-stranded M13mp18, allowing
262 extension up to the order of the kbp. We monitored primer extension activity for 30min at
263 55.5°C under 0.1, 10, 50 and 100MPa three times independently (Figure 3).

264

265 Curves showed a clear biphasic behavior at 0.1, 10 and 50MPa. Duration of the second
266 phase was reproducibly increased by HHP. In contrast, no clear biphasic behavior could be
267 observed at 100MPa.

268 Variability was higher in this experiment compared to strand displacement assays, as
269 indicated by larger standard deviation values, especially for the positive control (incubation at
270 P_{amb} for 2h prior to the fluorescence measurement to achieve maximal primer extension). As
271 with strand displacement experiments, fluorescence decreased over time. All other things
272 being equal, pressure tended to increase all curves, showing a putative effect of HHP on
273 intrinsic picogreen fluorescence or insertion in double-stranded DNA. Nonetheless, pressure-
274 inhibition of extension activity was still observable as the plateau was reached later, or not
275 reached at all, at 50 and 100MPa. The observed plateau unlikely resulted from dNTPs
276 depletion as they were provided in large excess and could have resulted instead from
277 unbounded picogreen shortage. In addition, maximum value of first derivative of the curves,
278 corresponding to the maximum increase of fluorescence, decreased with pressure and the
279 corresponding inflexion points, when applicable (0.1, 10 and 50MPa) were delayed
280 (Supplementary Figure 2).

281 To obtain more precise and quantitative information about the fluorescence variation
282 over time as a function of pressure, primer extension assays were replicated three times with
283 additional pressure values and with shorter acquisitions (15min). The curves were
284 transformed so that the value of fluorescence for positive control is equal to 100% and the
285 value of fluorescence for the negative control is equal to 0%, both at every instant. This way,
286 fluorescence was analyzed relative to controls and comparison between conditions was easier
287 (Supplementary Figure 3). By calculating first derivative of these curves, we then determined
288 relative increases of fluorescence as a function of time, roughly corresponding to elongation
289 speeds. Fastest increase in fluorescence over the whole experiment and punctual
290 fluorescence increase were calculated (Figure 4). Both maximum elongation efficiency
291 achieved during the whole 15min run and fluorescence increase at various moments of the
292 run were negatively affected by HHP above 10MPa. Milder pressure values (below 10MPa)
293 had little effect on fluorescence increase.

294

295 Effect of prior pressure treatment on *PabPolB* exo^- primer extension activity at ambient
296 pressure

297

298 To determine if the previously observed inhibiting effect of HHP on *PabPolB* exo^- was
299 irreversible or not, samples were incubated at 55.5°C and 100MPa during 15, 30 or 60min.
300 Upon decompression, measurement was immediately started and fluorescence was
301 measured for 15min. The experiment was done three times independently and average
302 relative fluorescence curves were determined (Figure 5).

303 Pre-incubation of the sample under HHP, even for longest durations, did not impair
304 significantly the primer extension activity of the enzymes when pressure was decreased to
305 ambient pressure. This shows that effect of pre-incubation on *PabPolB* *exo*⁻ activity was largely
306 reversible.

307

308 Comparison of pressure sensitivity of various thermostable DNA polymerases at 55.5
309 and 70.0°C

310

311 We then compared sensitivity to HHP of DNAPs from various organisms: *TaqPol* from
312 the thermophilic bacteria *Thermus aquaticus* and B-family DNAPs from hyperthermophilic
313 *Archaea*. Only *exo*⁻ mutants of archaeal DNAPs were used: *exo*⁻ *Pfu* Pol (Agilent) and Vent[®]
314 *exo*⁻ (NEB), respectively from *Pyrococcus furiosus* and *Thermococcus littoralis*, which have
315 both been isolated in a shallow water hydrothermal vents (Lundberg *et al.*, 1991; Kong *et al.*,
316 1993) and Deep Ven Vent[®] *exo*⁻ (NEB) from *Pyrococcus sp.* Strain GB-D , which has been
317 isolated in a 2km deep hydrothermal vent (Jannasch *et al.*, 1992), like *Pyrococcus abyssi*. All
318 archaeal enzymes had high sequence identity (Supplementary Figure 4).

319 Primer extension activity was measured during 30min three times independently for
320 each enzyme at 0.1, 10, 50 and 100MPa, at 55.5 or 70.0°C. For reactions at 70.0°C, single-
321 stranded m13mp18 was annealed to a longer primer (87nt rather than 30nt) to prevent
322 melting of the hybrid. Curves were transformed as described previously and average
323 maximum fluorescence increase observed during the whole run was determined. For each
324 enzyme, the value at 0.1MPa was set to 100% in order to compare their elongation efficiency
325 independently (Figure 6).

326 All commercial archaeal enzymes showed gradual inhibition by HHP at both 55.5 and
327 70.0°C. However, increasing the temperature compensated the decrease of activity induced
328 by HHP. *Taq* enzyme turned to be more pressure-tolerant at 70.0°C than Vent[®] *exo*⁻ and Deep
329 Vent[®] *exo*⁻. At 55.5°C, Deep Vent[®] *exo*⁻ was the most pressure-sensitive DNAP as dramatical
330 decrease of maximum achieved elongation speed already started at 10MPa. In contrast, *Pfu*
331 *exo*⁻ DNAP showed reduced inhibition by HHP in most conditions compared to the other
332 commercial archaeal enzymes. However, *Pfu* *exo*⁻ was the only enzyme used in the
333 commercial buffer which contained triton X-100.

334 Unlike what was observed at 55.5°C, maximum elongation speed of *PabPolB* *exo*⁻ was
335 significantly increased at both 10 and 50MPa when reaction occurred at 70.0°C. None of the
336 other tested enzymes showed such behavior. Moreover, at such temperature the maximum
337 observed speed was only halved by 100MPa exposure.

338 Discussion

339

340 We have showed here for the first time that, unlike many enzymes from both
341 extremophiles and non-extremophiles whose activities can be enhanced by HHP
342 (Eisenmenger and Reyes-De-Corcuera, 2009), DNA polymerase are inhibited by HHP above
343 10MPa. Effects of HHP on proteins are rather complex and depend on the protein. As a general
344 rule, response to pressure is governed by Le Chatelier's principle which predicts that a system
345 at the equilibrium will respond to an increase of pressure through a decrease of volume
346 (Heremans, 2009; Jebbar *et al.*, 2015). For proteins, this decrease may result from two distinct
347 effects: reversible compression, especially for proteins with large internal cavities, and
348 unfolding which allows additional condensation of water molecules (Doster *et al.*, 2003;
349 Eisenmenger and Reyes-De-Corcuera, 2009). At 400MPa, most proteins are, hence, fully
350 unfolded (Aertsen *et al.*, 2009). Dissociations of molecular assemblies, such as the ribosome
351 (Pande and Wishnia, 1986; Gross *et al.*, 1993), are also promoted under HHP as it releases
352 sites for water condensation, most assemblies being fully dissociated at 200MPa (Aertsen *et al.*,
353 2009). Yet, it is not possible to impute the observed HHP inhibition of DNAPs on unfolding.
354 In particular, the post-pressurization experiments show that, whatever its cause, the nearly
355 full inhibition at 100MPa was reversible, just like what was observed with a RNA polymerase
356 from a non-thermophilic abyssal bacteria (Kawano *et al.*, 2004).

357 While gel analysis of primer extension products provides a simple way to assess effects
358 of HHP on DNA polymerization activity, the fact that this analysis can only be made after
359 decompression may bias the results as fast pressure change could have specific effects such
360 as sudden and quick stimulation of primer extension. Nonetheless, these experiments showed
361 that the decrease of total elongated DNA synthesized by *PabPolB* exo^- was observable from
362 50MPa at 55.5°C and from 25MPa at 65.0°C, showing that pressure inhibition of DNAPs activity
363 depends on temperature, as confirmed by the primer extension assays. It should also be
364 pointed that *PabPolB* could realize rolling circle replication of which requires displacement of
365 elongated primer and, hence, relies on strand displacement activity which we showed to be
366 inhibited by HHP. Such effect could contribute, to some extent, to the observed inhibition.

367 In contrast, it has been showed that HHP, up to 89MPa, actually increase
368 thermostability of both DNAPs of *Pyrococcus* strains and *Taq* DNAP (Summit *et al.*, 1998).
369 Hence, the HHP inhibition may result instead from subtle changes in protein structures and
370 dynamics enhancing stability at the expense of activity. Psychrophilic enzymes, which present
371 flexibility-inducing traits, may therefore be less sensitive to pressure inhibition. However, no
372 experimental comparison of pressure-sensitivity between homologous thermophilic,
373 mesophilic and psychrophilic deep-sea enzymes has been published, to our knowledge.
374 Nonetheless, synergy between psychrophilic and piezophilic protein traits has been pointed
375 (Capece *et al.*, 2013; Carré *et al.*, 2022).

376 Strand displacement activity assays were limited by the fact that interaction between
377 the DNA template and quencher-harboring oligonucleotide is sensitive to pressure. While
378 short simple double stranded DNA fragments can be destabilized by HHP (Hughes and Steiner,
379 1966; Gunter and Gunter, 1972), HHP actually tend to increase stability of DNA hybrids
380 (Macgregor, 1996; Rayan and Macgregor, 2005). Therefore, if no interference caused by the
381 Deep Dark Quencher I 3'-modification and 6-FAM fluorophore is assumed, interaction
382 between the oligonucleotides was reinforced under HHP. Hence, in addition to any direct

383 effect on the enzyme, strand displacement activity was inhibited by the strengthened
384 interaction between the DNA template and the strand that the enzyme had to displace.
385 Indeed, total inhibition at 100MPa was observed during strand displacement assays whereas
386 some activity could still be observed during primer extension assay. Therefore, assays that
387 directly measure extension activity should be preferred to more indirect methods for HHP
388 studies of DNAPs. One should notice that at higher temperatures the decreased stability of
389 double-stranded DNA could compensate for HHP inhibition of strand displacement activity.

390 The biphasic behavior observed in primer extension activity curves is consistent with
391 the biphasic model of DNAPs enzymatic activity. In such model, the first short phase
392 corresponds to the addition of the first dNTP to the primer by all enzymes which is faster than
393 the following dNTP polymerizations, which correspond to the second phase (Berdis, 2009).
394 Our data suggest that this second phase is more affected by HHP as the quick initial increase
395 of fluorescence was observed at 10 and 50MPa while the second more gradual increase
396 appeared to be delayed at these pressure values and was mostly absent at 100MPa. This
397 stresses the hypothesis that HHP impairs DNAPs activity through direct inhibition of primer
398 extension rather than substrate binding.

399 Surprisingly high tolerance to HHP was observed with *Taq* DNAP, which originates from
400 *Thermus aquaticus*, a surface thermophilic bacterium. Since *T. aquaticus* is less thermophilic
401 than the archaea from which the other tested DNAPs were from, its proteins may be less
402 thermostable, thus less resilient and less rigid (Aguilar *et al.*, 1997; Tehei and Zaccai, 2007;
403 Zaccai, 2013), which could explain its low sensibility to HHP. However, *Taq* is A-family DNAP
404 whereas all the other tested enzymes are from the B family. Depending on the fold and
405 especially the internal cavities, intrinsic flexibility and, hence, sensitivity to HHP could vary
406 between DNAP families.

407 When compared to the other exo⁻ B-family archaeal DNAPs, *PabPolB* showed increased
408 tolerance to HHP. As little sequence variation is observed between these enzymes, subtle
409 structural changes, at the level of internal cavities or interdomain hinges, may explain these
410 differences. *PabPolB* exo⁻ was the only tested enzyme that was not purchased but produced
411 and purified by us. In general, little information about piezophilic adaptation can be inferred
412 from protein sequences as they are mostly dictated by temperature in abyssal environments
413 (hot hydrothermal vents or cold waters and sediments) (Nath and Subbiah, 2016).
414 Nonetheless, in comparison to their non-piezophilic homologs, enzymes from deep-sea
415 organisms tend to have denser cores with smaller residues, less salt bridges (Carré *et al.*,
416 2022).

417 Still, increasing temperature compensated HHP inhibition of all tested enzymes. This
418 could result from two separate causes. First, the evaluated enzymes are hyperthermophilic,
419 their optimal temperature being between 72 and 80°C for archaeal DNAPs (Zhang *et al.*, 2015),
420 increasing the temperature from 55.5 to 70.0°C may hence be sufficient to account for the
421 increase of the maximum elongation speed. Second, temperature may directly reduce the
422 inhibiting effects of HHP through the increase of molecular motion and flexibility (Daniel and
423 Cowan, 2000). Nonetheless, the present work stresses the importance of heat sources in deep
424 environments where organisms are constantly under HHP. This is especially true for putative
425 extraterrestrial abysses which could be deeper and exposed to pressure values above 100MPa
426 (Naganuma and Uematsu, 1998).

427 Pressure adaptation of abyssal microorganisms still remains unclear. In particular,
428 complex processes such as DNA replication can be affected by HHP in a complex manner as it

429 involves multiple protein, multimeric assemblies, proteins and DNA. Moreover, care should
430 be taken when extrapolating data obtained *in vitro* on simple protein systems studied in
431 buffers of given composition to the physiological intracellular context. Cytoplasmic crowding,
432 interactions with piezolytes or with the other replisome proteins may indeed limit the effects
433 of HHP on DNAPs. While HHP tend to disrupt multimeric assemblies and, hence, could impair
434 replisome formation, depending on the volumetric parameters of each protein-protein and
435 protein-DNA interaction, GINS or PCNA complexes could limit pressure-sensitivity of DNAPs.
436 In particular, it has been shown that addition of PCNA improves strand displacement activity
437 (Henneke *et al.*, 2005) and fidelity (Castillo-Lizardo *et al.*, 2014) of *PabPolB in vitro*.

438

439 DNAPs could work better within the replisome by interacting with, for example, GINS
440 or PCNA complexes. . In particular, interactions with GINS or PCNA complexes

441 Nonetheless, the deepest hydrothermal vents on Earth are found at a depth of 5km
442 and most are found above 2km deep, limiting the pressure conditions to which such these
443 organisms are actually exposed. Another possibility could be that high temperatures are
444 sufficient to compensate inhibitory effects of HHP. Indeed, most of our experiments were
445 made at 55.5°C, which is below the temperature range at which *Thermococcales* species such
446 as *P. abyssi* grow (Erauso *et al.*, 1993).

447 This could stress even more the dependency on temperature of abyssal
448 hyperthermophilic microorganisms and the need to search for heat sources in the
449 extraterrestrial deep oceans.

450 Conclusion

451 In this work, effects of high hydrostatic pressure (HHP) on DNA polymerases (DNAPs)
452 of abyssal and surface (hyper)thermophilic microorganisms was explored for the first time. By
453 using various fluorescence-based approaches, including real-time fluorimetric assays, we
454 showed that HHP inhibits total DNA synthesis, strand displacement activity and extension
455 rate. These effects were showed to be reversible, mitigated by higher temperature and
456 dependent on the enzymes.

457

458 Acknowledgements

459

460 This work is supported by the French National Research Agency in the framework of
461 the Investissements d'Avenir program (ANR-15-IDEX-02), through the funding of the "Origin
462 of Life" project of the Univ. Grenoble-Alpes.

463 IBS acknowledges integration into the Interdisciplinary Research Institute of Grenoble
464 (IRIG, CEA).

465 High-pressure experiments were conducted with the BioHP platform of the IBS.

466

467 Author contributions

468

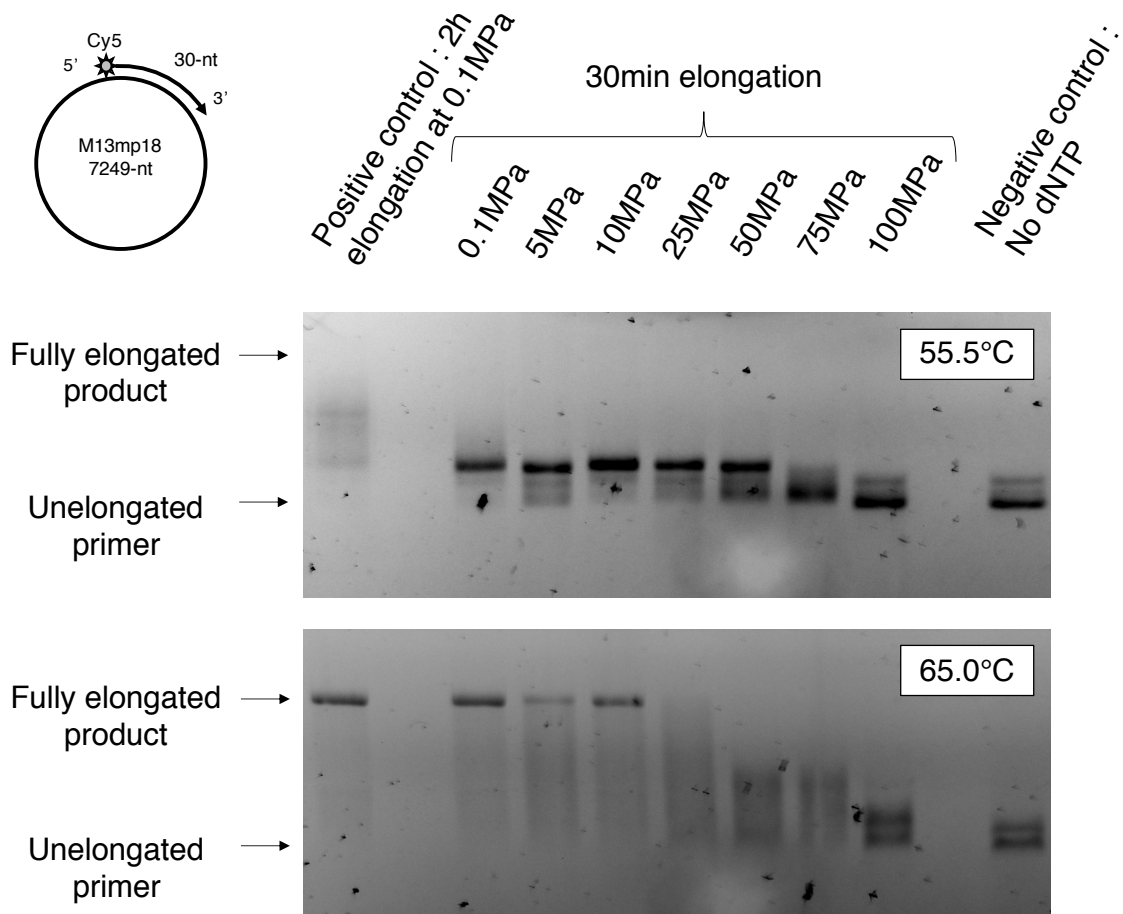
469 All authors proposed and contributed in their respective expertise and participated in
470 writing the manuscript. L.C. designed research, conducted experiments, analyzed data, wrote
471 the paper and made the figures, G.H., E.H. and D.F. designed research and corrected the
472 paper, E.G. and B.F. designed research, wrote and corrected the paper.

473

474 Disclosure statement

475

476 The authors are not aware of any affiliations, memberships, funding, or financial
477 holdings that might be perceived as affecting the objectivity of this review.

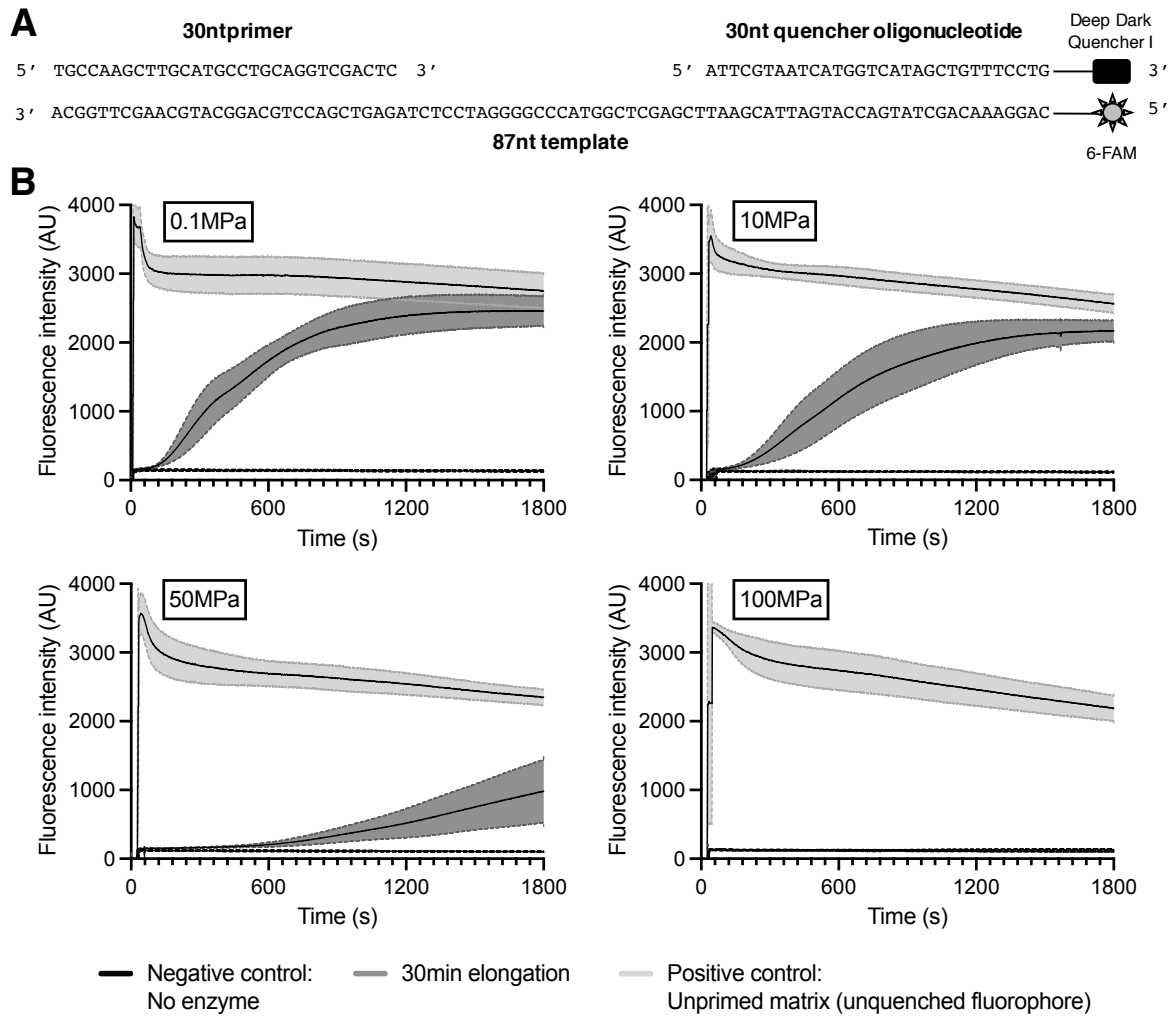


478

479

480 Figure 1: Gel analysis of products of *PabPolB* exo⁻ under HHP

481 Extension of the Cy5-labeled 30nt long primer hybridized on a m13MP18 DNA template of
 482 7249nt in length under pressure values indicated above and temperatures indicated on the
 483 left.

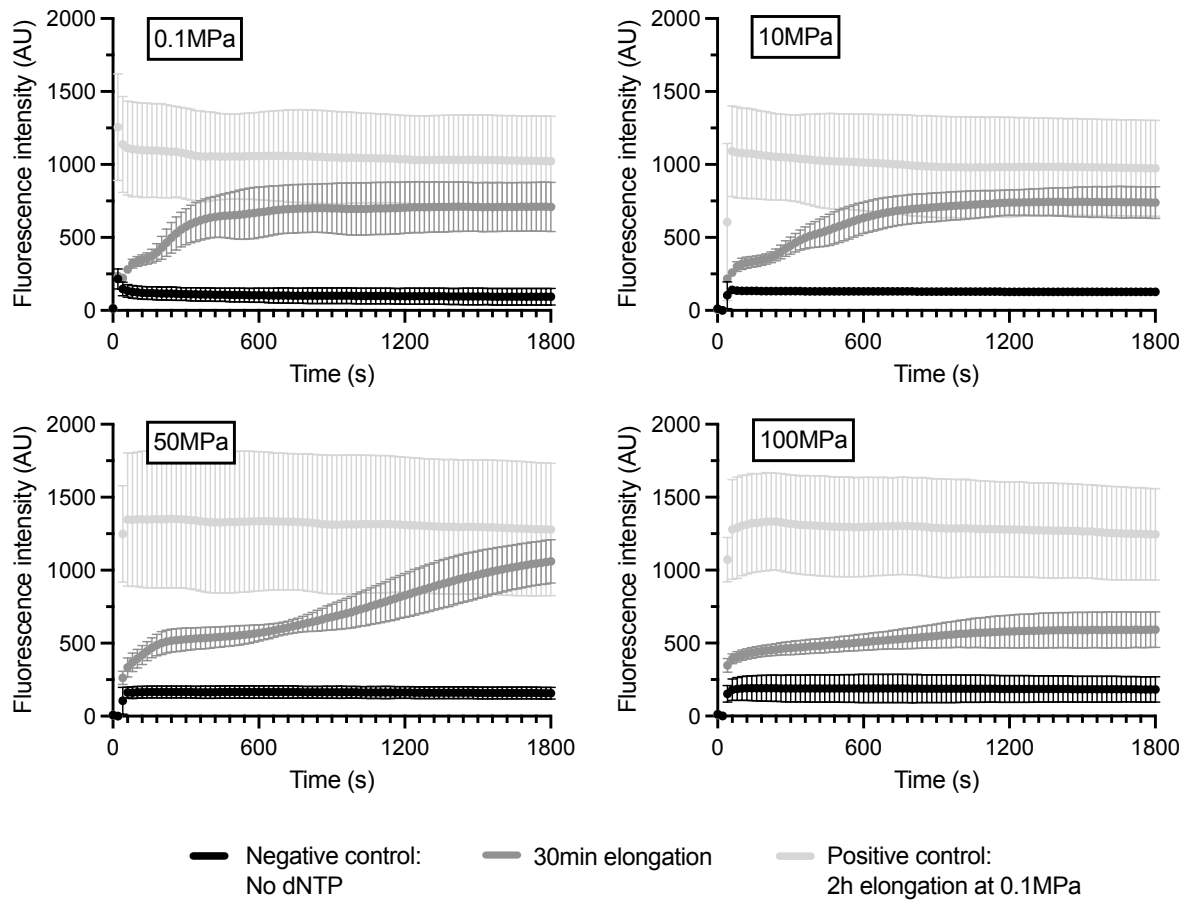


484

485

486 Figure 2: Realtime monitoring of strand displacement activity of *PabPolB* exo^- under HHP

487 A: tripartite DNA hybrid used for these experiments consists of a 87nt template labelled at the
 488 5' end with a 6-FAM modification hybridized to a 30nt primer and to a 30nt oligonucleotide
 489 labelled with a Deep Dark Quencher I modification at the 3' end. Unless this oligonucleotide
 490 is removed, the fluorescence of the 6-FAM is quenched. B: strand displacement activity of
 491 *PabPolB* exo^- under various pressure conditions. The curves represent the average
 492 fluorescence over three independent experiments and the colored area corresponds to the
 493 standard deviation. Controls are indicated.

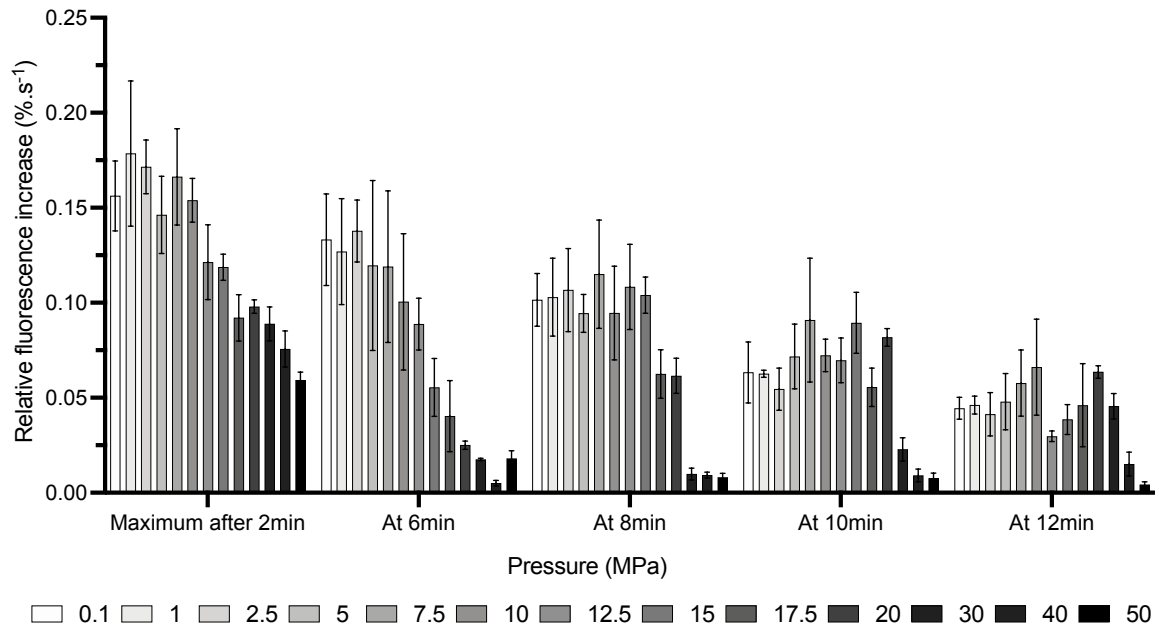


495

496

497 Figure 3: Realtime monitoring of primer extension activity of *PabPolB* exo^- under HHP

498 Fluorescence signal of picogreen intercalant during the extension of the unlabelled 30nt long
 499 primer hybridized on a m13MP18 DNA template. The curves represent the average
 500 fluorescence over three independent experiments and the colored area corresponds to the
 501 standard deviation. Controls are indicated.



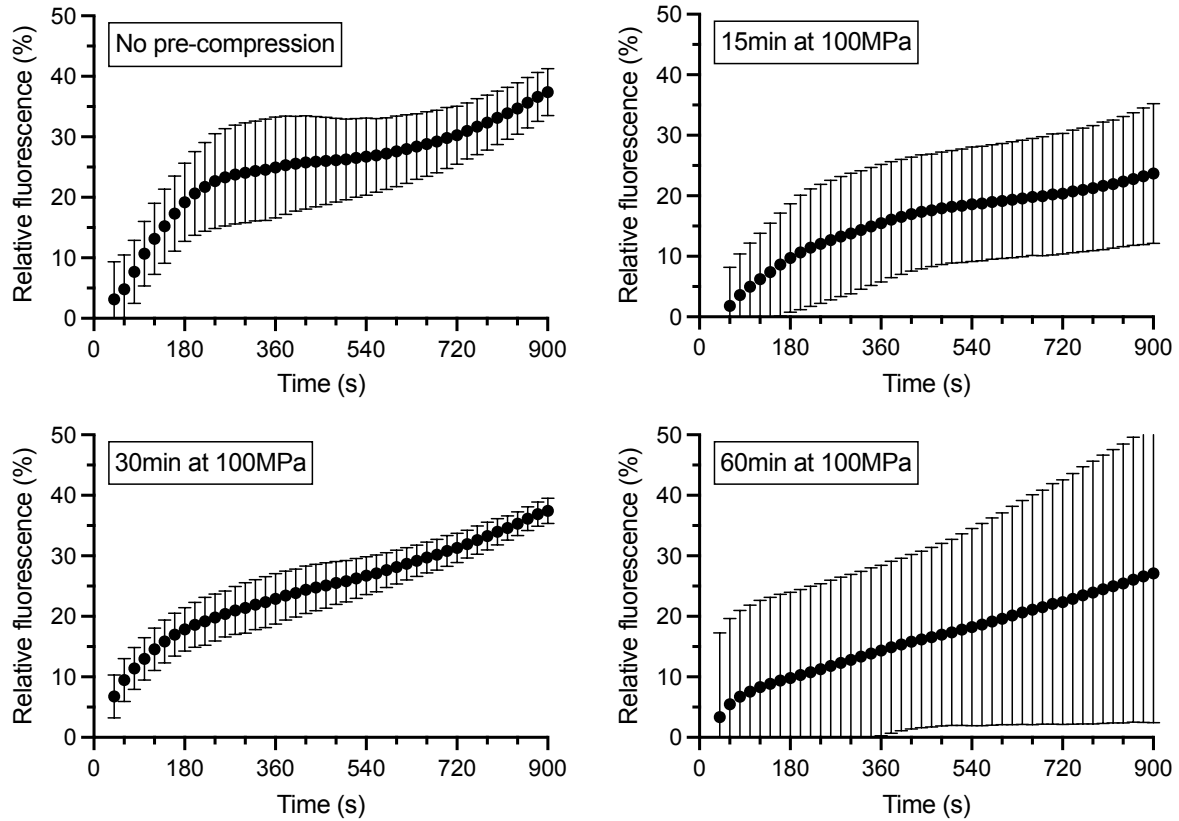
502

503

504 Figure 4: Effect of HHP on elongation speed of *PabPolB* exo^-

505 Primer extension curves were normalized using positive and negative controls as, respectively,
 506 superior and inferior limits. First derivatives were calculated for each of the three
 507 independently obtained curves. Error bars correspond to standard deviation. Colors represent
 508 pressure value (see legend).

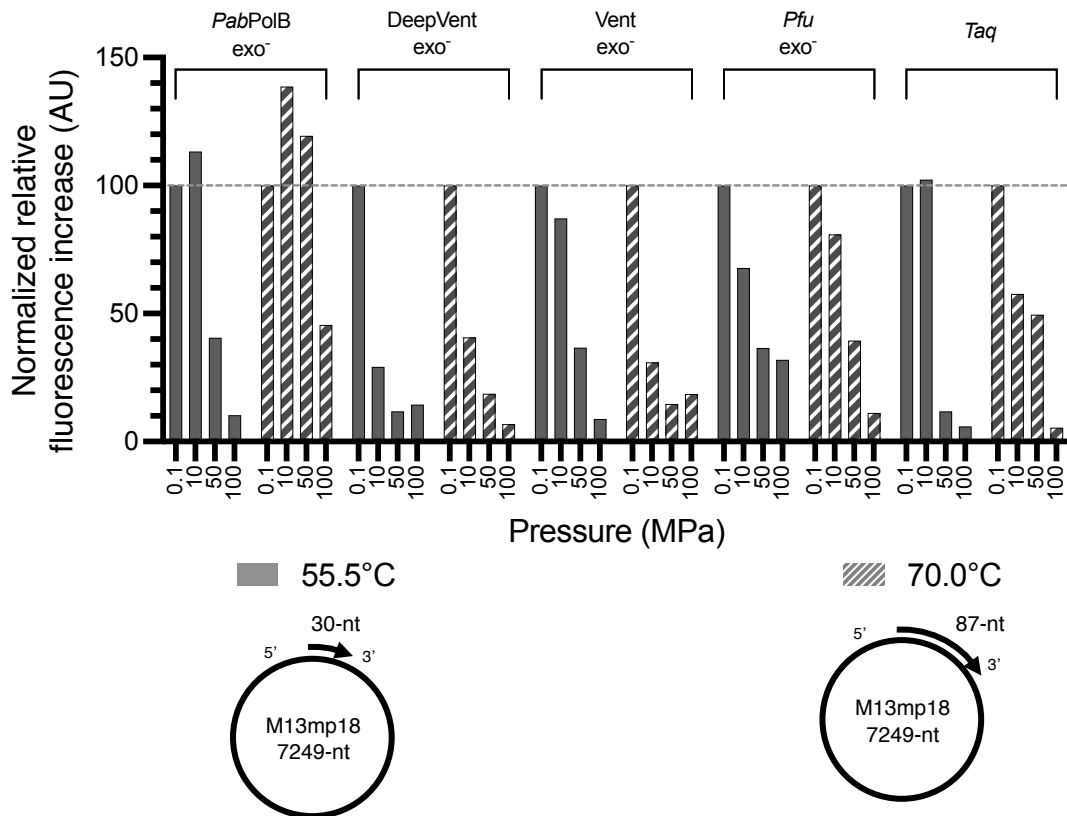
509



510

511 Figure 5: Effect of pre-compression on primer extension activity of *PabPolB* exo^- at P_{amb}

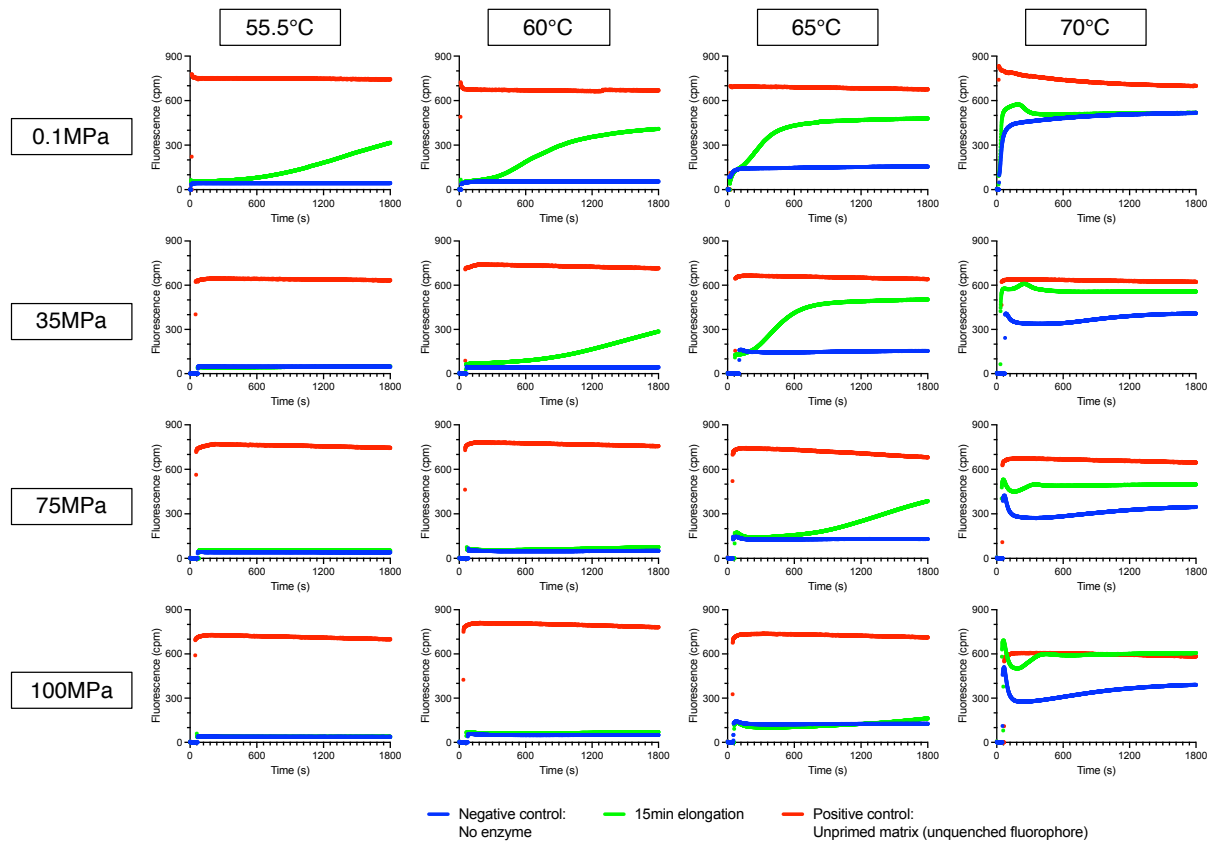
512 Primer extension curves were normalized using positive and negative controls as, respectively,
 513 superior (100%) and inferior (0%) limits. The curves represent the average fluorescence over
 514 three independent experiments. Incubation under HHP prior to fluorescence measurement is
 515 indicated. Error bars represent standard deviation.



516

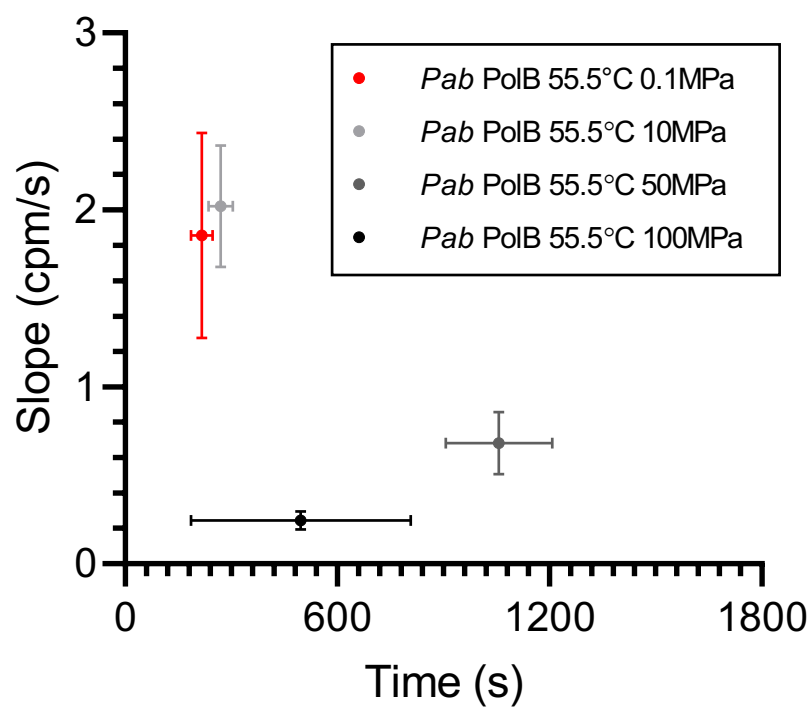
517 Figure 6: Comparison of pressure-sensitivity of various DNAPs

518 Primer extension curves were normalized using positive and negative controls as, respectively,
 519 superior and inferior limits. First derivatives were calculated for each of the three
 520 independently obtained curves. Average maximum observed speed is plotted as a function on
 521 the enzyme and pressure/temperature combination. To facilitate observation of the effect of
 522 HHP on elongation speed, for each temperature and enzyme, maximum speed at 0.1MPa was
 523 set to 100% and speeds at the other pressure values were compared to them. DNA template-
 524 primer hybrids used in each temperature condition are schematically represented below
 525 legend.



Supplementary Figure 1: Effect of HHP on strand displacement activity of *PabPolB* exo^- at various temperatures

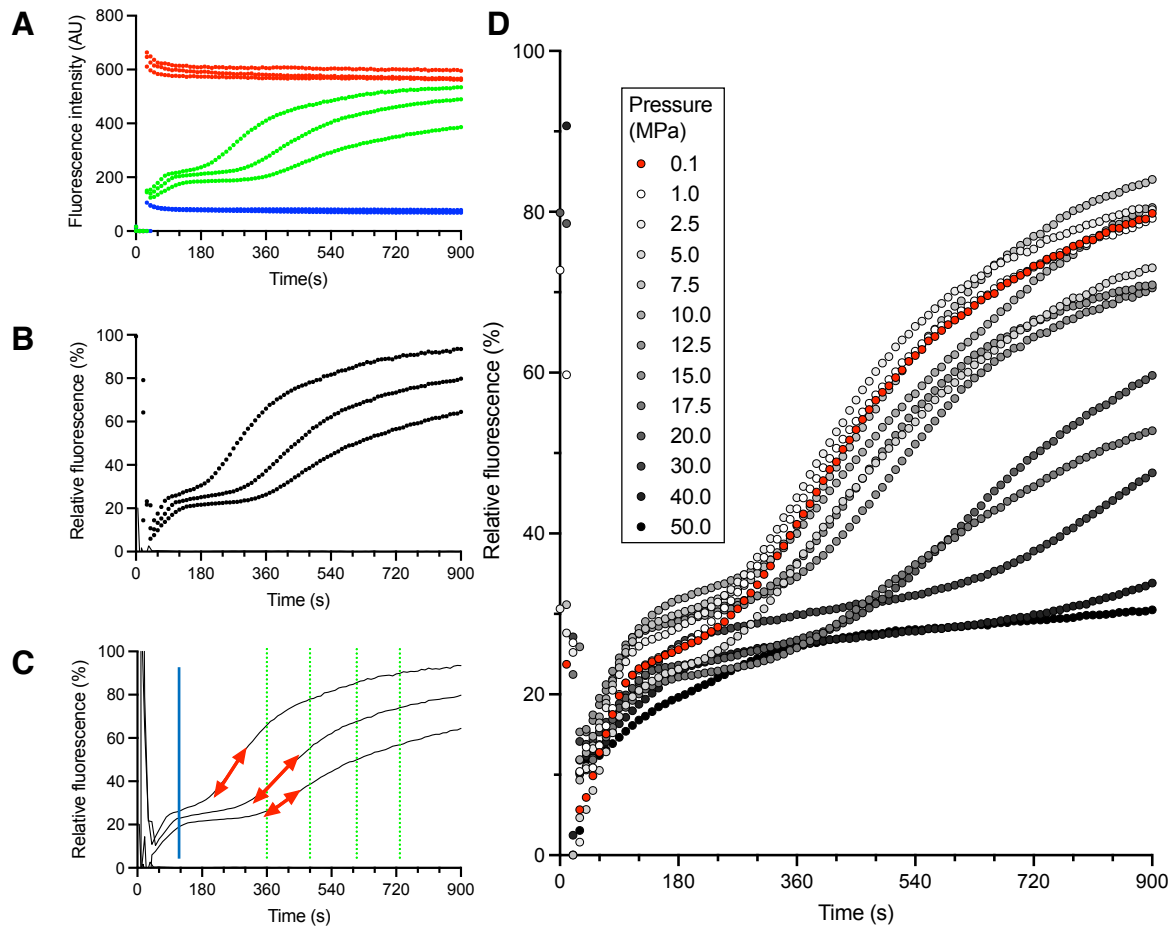
Fluorescence signal of the 6-FAM fluorophore harboured by the 87nt long DNA template increasing as the 30nt long oligonucleotide modified with a Deep Dark Quencher I is displaced by the enzyme. Curves were obtained only once. Controls are indicated. Notice that signal of the negative control at 70.0°C increases with heat as a consequence of spontaneous denaturation of DNA.



536

537 Supplementary Figure 2: Position and value of maximum fluorescence increase during primer-
 538 extension assays

539 Bars represent standard deviation. As no biphasic behaviour could be observed at 100MPa,
 540 only values obtained at 0.1, 10 and 50MPa correspond to an inflexion point.



542

543 Supplementary Figure 3: HHP relative primer extension curves of *PabPolB exo⁻*

544 A: Raw data for extension curves (green), positive (red) and negative (blue) controls,
 545 corresponding to the three independent measurements made at 1MPa and 55.5°C. B: relative
 546 fluorescence curves, based on raw data depicted in A, made using positive and negative
 547 controls as, respectively, superior (100%) and inferior (0%) limits. C: red arrows indicate
 548 localization of maximum value, after equilibration of pressure and temperature (blue line), of
 549 first derivative of relative fluorescence, corresponding to the maximum elongation speed;
 550 green dotted lines indicate additional timepoints at which values of first derivative were
 551 retrieved to be plotted in Figure 4. D: average relative fluorescence curves calculated over
 552 three independent experiments for every tested pressure values.

Vent_exo+	MILDYITDKGPIIRIFKKEGEFKIELDPHFQPIYIALLKDDSAIEEIKAIKERHG	60
Pfu_exo+	MILDVDYITEEGKPVIRLFFKKENGKFKIEHDFRFRPIYIALLRDDSKIEEVKITGERHG	60
Pab_exo+	MILDADYITEDGKPIIRIFKKEKGEFKVEYDRFRFRPIYIALLKDDSAIDEVKITAERHG	60
Deep_Vent_exo+	MILDADYITEDGKPIIRIFKKEGEFKVEYDRFRFRPIYIALLKDDSQIDEVKITAERHG	60
	* ** : . : * : * : * : * : * : * : * : * : * : * : * : * : * : * : * : * : *	
Vent_exo+	KTVRVLDAVKVRKFLGREVEVKLIFEPQDVPAHRGKIREHPAVVDIYEYDIPFAKRY	120
Pfu_exo+	KIVRIVDVEKVEKFLGKPIVWKLYLEHPQDVPTIREKVEHPAVVDIFEYDIPFAKRY	120
Pab_exo+	KIVRIVTEVKVQKFLGRPIEVWKLYLEHPQDVPAIREKIREHPAVVDIFEYDIPFAKRY	120
Deep_Vent_exo+	KIVRIDA EKVRKFLGRPIEVWRLYFEPQDVPAIRDKIREHSAVIDIFEYDIPFAKRY	120
	* ** : . : * : * : * : * : * : * : * : * : * : * : * : * : * : * : * : * : *	
Vent_exo+	LIDKGLIPMEGDEELKLLAFDIETFYHGEFEGKGEIIMISYADEEEARVITWKNDLPHY	180
Pfu_exo+	LIDKGLIPMEGEELKLLAFDIETLYHGEFEGKGIIMISYADENEAKVITWKNDLPHY	180
Pab_exo+	LIDKGLTPMEGNEELTFLAVDIETLYHGEFEGKGIIMISYADEEGAKVITWKSIDLPHY	180
Deep_Vent_exo+	LIDKGLIPMEGDEELKLLAFDIETLYHGEFEGKGIIMISYADEEEAKVITWKKIDLPHY	180
	***** * : : * : * : * : * : * : * : * : * : * : * : * : * : * : * : * : *	
Vent_exo+	VDVVSNEREMIKRFRVQVVKDKDPVVIITNGDNFDLPYLKRAEKLGRVLLVGRDKEHPE	240
Pfu_exo+	VEVVSSEREMIKRFLRIIREKDPDIIVTNGDSDFPFLAKRAEKLGIKLIGRGG—SE	238
Pab_exo+	VEVVSSEREMIKRLVKVIREKDPDVIITNGDNFDFPYLLKRAEKLGIKLPLGRDN—SE	238
Deep_Vent_exo+	VEVVSSEREMIKRFLKVIIEKDPDVIITNGDSDFLPYLKRAEKLGIKLPLGRD—SE	238
	* ** : . : * : * : * : * : * : * : * : * : * : * : * : * : * : * : * : * : *	
Vent_exo+	PKIQRMGDSFAVEIKGRIFHFDLPVVRRTINLPTYTLEAVYEAFLGKTKSKLGAEEIAAI	300
Pfu_exo+	PKMQRIGDMTAVEVKGRIHFDLHVYVTRINLPTYTLEAVYEAIFGKPKKPYAIDEIAKA	298
Pab_exo+	PKMQRMGDSLAVEIKGRIFHFDLPVVRRTINLPTYTLEAVYEAIFGSKKPYAIEAEA	298
Deep_Vent_exo+	PKMQRLGDMTAVEIKGRIFHFDLHVYVTRINLPTYTLEAVYEAIFGKPKKYAIEAEA	298
	* ** : * : * : * : * : * : * : * : * : * : * : * : * : * : * : * : * : *	
Vent_exo+	WETEESMKKLAQYSMEDARATYELGKFFPMEAELAKLIGQSVWDVSRSSGNLVEWYLL	360
Pfu_exo+	WESGENLERVAKYSMEDAKATYELGKFEFLPMIQLSRLVGPQWLVSRSSGNLVEWYLL	358
Pab_exo+	WETGKGLERVAKYSMEDAKVTFELGKFFPMEAQLARLVGPQWLVSRSSGNLVEWYLL	358
Deep_Vent_exo+	WETGKGLERVAKYSMEDAKVTYELGKFFPMEAQLSRLVGPQWLVSRSSGNLVEWYLL	358
	* ** : . : : * : * : * : * : * : * : * : * : * : * : * : * : * : * : * : * : *	
Vent_exo+	RVAYARNELAPNKPDEEYKRRRTTLYGGYVKEPEKGLWENIYLDFRSLYPSIIVTHN	420
Pfu_exo+	RKAYERNEVAPNKPSEEEYQRRRESYTGGFVKPEKGLWENIVYLDFRALYPSIITHN	418
Pab_exo+	RKAYERNELAPNKPDEREYRRLRESYEGGYVKEPEKGLWEGIVSLDFRSLYPSIITHN	418
Deep_Vent_exo+	RKAYERNELAPNKPDEREYERRRESYAGGYVKEPEKGLWEGVSLDFRSLYPSIITHN	418
	* ** * : * : * : * : * : * : * : * : * : * : * : * : * : * : * : * : * : *	
Vent_exo+	VSPDTLEKEGCKNYDVAIVGYRFCKDFPFIPLGDLIAMRQDIKMKKSTIDPIEKK	480
Pfu_exo+	VSPDTLNLGCKNYDIAPIQVGHKFKDIPGFIPSLGLLEERQKIKTKMKETQDPIEKI	478
Pab_exo+	VSPDTLNLRENCKEYDVAIQVGHKFKDFPFIPLGDLNLEERQKIKKRMKESKDPVEKK	478
Deep_Vent_exo+	VSPDTLNLREGCREYDVAIVEGHKFKDFPFIPLLLKRLDERQEKIKMKASKDPPIEKK	478
	***** * : * : * : * : * : * : * : * : * : * : * : * : * : * : * : * : *	
Vent_exo+	MLDYRQRAIKLLANSYGYMGYPKARWYKCAESVTAWGRHYIEMTIREIEEKFGFKVL	540
Pfu_exo+	LLDYRQKAIKLLANSFYGYGYAKARWYKCAESVTAWGRKYIELVWKELEKFGFKVL	538
Pab_exo+	LLDYRQRAIKLLANSYGYGYAKARWYKCAESVTAWGRQYIDLVRRELES—RGFKVL	537
Deep_Vent_exo+	MLDYRQRAIKLLANSYGYGYAKARWYKCAESVTAWGREYIEFVRKELEKFGFKVL	538
	: ***** * : * : * : * : * : * : * : * : * : * : * : * : * : * : * : *	
Vent_exo+	YADTDGFIATIPGKEPELIKKAKEFLNYINSKLPGLLELEYEGFYLGRFFVTKKRYAVI	600
Pfu_exo+	YIDTDGLYATIPGGSEEEIKKALEFVKYINSKLPGLLELEYEGFYKRGFFVTKKRYAVI	598
Pab_exo+	YIDTDGLYATIPGAKHEEIKKALKFVEYINSKLPGLLELEYEGFYARGFFVTKKRYALI	597
Deep_Vent_exo+	YIDTDGLYATIPGAKPEEIKKALEFVDYINAKLPGLLELEYEGFYVRFVVTKKRYALI	598
	* ** : * : * : * : * : * : * : * : * : * : * : * : * : * : * : * : * : *	
Vent_exo+	DEEGRIITRGLVVRDSEIAKETQAKVLEAILKGGVEKAVEVVRDVVEKIAKRYRVL	660
Pfu_exo+	DEEGKIVTRGLEIVRRDSEIAKETQARVLEILKHGDVEEAIRIVKEVIKLANEYIPP	658
Pab_exo+	DEEGKIVTRGLEIVRRDSEIAKETQAKVLEAILKHGNVDEAVKIVKEVTEKLSKYEIPP	657
Deep_Vent_exo+	DEEGKIITRGLEIVRRDSEIAKETQAKVLEAILKHGNVEEAIVKEVTEKLSKYEIPP	658
	***** : ***** * : * : * : * : * : * : * : * : * : * : * : * : * : *	
Vent_exo+	EKLVIHEQITRDLDYKAI GPHVAIAKRLAARGIKVPGTII SYIVLKGSGKISDRVILL	720
Pfu_exo+	EKLAIYEQITRPLHEYKAI GPHVAVAKLAAKGVKIPGMVIGYIVLRGDGPISNRAILA	718
Pab_exo+	EKLVIYEQITRPLSEYKAI GPHVAVAKLAAKGVKVPGMVIGYIVLRGDGPISKRAIAI	717
Deep_Vent_exo+	EKLVIYEQITRPLHEYKAI GPHVAVAKLAAKGVKVRPDMVIGYIVLRGDGPISKRAIALA	718
	*** : ***** * : ***** * : * : * : * : * : * : * : * : * : * : *	
Vent_exo+	TEYDPRKHKYDPDIYIENQVLPVLRILEAFGYRKEMLRYQSSKQTGLDAWLKR---	774
Pfu_exo+	EEYDPKKHKYDAEYIENQVLPVLRILEFGYRKEMLRYQKTRQVGLTSLWLNKKS	775
Pab_exo+	EEFDPKKHKYDAEYIENQVLPVLRIRAFGYRKEMLRYQKTRQVGLGAWLKF---	771
Deep_Vent_exo+	EEFDLRRKHKYDAEYIENQVLPVLRILEAFGYRKEMLRWQKTRQVGLTAWLNIKKS	775
	* ** : ***** : ***** * : * : * : * : * : * : * : * : * : * : *	

553

554 Supplementary Figure 4: Sequence alignments between exo⁺ forms of tested archaeal
555 enzymes

556 Since sequences of exo⁻ mutants of commercial enzymes were unknown, intein-free
557 sequences of wild-type exo⁺ enzymes were compared instead. Sequences of

558 *Pyrococcus* specie GB-D, *Thermococcus littoralis* and *Pyrococcus furiosus* PolB present
559 sequence identity to *P. abyssi* PolB of 89.4%, 76.3% and 83.8%, respectively.

560 References

561

562 Abe, F., Kato, C., Horikoshi, K. (1999). Pressure-regulated metabolism in microorganisms.
563 *Trends in Microbiology* 7:447–453.

564 Aertsen, A., Meersman, F., Hendrickx, M.E.G., Vogel, R.F., Michiels, C.W. (2009).
565 Biotechnology under high pressure: applications and implications. *Trends in Biotechnology*
566 27:434–441.

567 Aguilar, C.F., Sanderson, I., Moracci, M., Ciaramella, M., Nucci, R., Rossi, M., Pearl, L.H.
568 (1997). Crystal structure of the β -glycosidase from the hyperthermophilic archeon *Sulfolobus*
569 *solfataricus*: resilience as a key factor in thermostability¹¹Edited by R. Huber. *Journal of*
570 *Molecular Biology* 271:789–802.

571 Anderson, J.D., Lau, E.L., Sjogren, W.L., Schubert, G., Moore, W.B. (1997). Europa's
572 Differentiated Internal Structure: Inferences from Two Galileo Encounters. *Science*
573 276:1236–1239.

574 Anderson, J.D., Schubert, G., Jacobson, R.A., Lau, E.L., Moore, W.B., Sjogren, W.L. (1998).
575 Europa's Differentiated Internal Structure: Inferences from Four Galileo Encounters. *Science*
576 281:2019–2022.

577 Belilla, J., Moreira, D., Jardillier, L., Reboul, G., Benzerara, K., López-García, J.M., Bertolino,
578 P., López-Archilla, A.I., López-García, P. (2019). Hyperdiverse archaea near life limits at the
579 polyextreme geothermal Dallol area. *Nat Ecol Evol* 3:1552–1561.

580 Berdis, A.J. (2009). Mechanisms of DNA Polymerases. *Chem Rev* 109:2862–2879.

581 Cable, M.L., Clark, K., Lunine, J.I., Postberg, F., Reh, K., Spilker, L., Waite, J.H. (2016).
582 Enceladus Life Finder: the search for life in a habitable moon.

583 Canceill, D., Viguera, E., Ehrlich, S.D. (1999). Replication Slippage of Different DNA
584 Polymerases Is Inversely Related to Their Strand Displacement Efficiency. *J Biol Chem*
585 274:27481–27490.

586 Carré, L., Zaccai, G., Delfosse, X., Girard, E., Franzetti, B. (2022). Relevance of Earth-Bound
587 Extremophiles in the Search for Extraterrestrial Life. *Astrobiology* 22:322-367.

588 Castillo-Lizardo, M., Henneke, G., Enrique, V. (2014). Replication slippage of the thermophilic
589 DNA polymerases B and D from the Euryarchaeota *Pyrococcus abyssi*. *Frontiers in*
590 *Microbiology* 5:403.

591 Connelly, D.P., Copley, J.T., Murton, B.J., Stansfield, K., Tyler, P.A., German, C.R., Dover,
592 C.L.V., Amon, D., Furlong, M., Grindlay, N., Hayman, N., Hühnerbach, V., Judge, M., Bas, T.L.,
593 McPhail, S., Meier, A., Nakamura, K., Nye, V., Pebody, M.)? , Pedersen, R.B., Plouviez, S.,
594 Sands, C., Searle, R.C., Stevenson, P., Taws, S., Wilcox, S. (2012). Hydrothermal vent fields
595 and chemosynthetic biota on the world's deepest seafloor spreading centre. *Nat Commun*
596 3:1–9.

597 Daniel, R.M., Cowan, D.A. (2000). Biomolecular stability and life at high temperatures.
598 *Cellular and Molecular Life Sciences CMLS* 57:250–264.

599 Dorjsuren, D., Wilson, D.M., Beard, W.A., McDonald, J.P., Austin, C.P., Woodgate, R., Wilson,
600 S.H., Simeonov, A. (2009). A real-time fluorescence method for enzymatic characterization of
601 specialized human DNA polymerases. *Nucleic Acids Research* 37:e128–e128.

602 Doster, W., Gebhardt, R., Soper, A.K. (2003). Pressure-induced Unfolding of Myoglobin:
603 Neutron Diffraction and Dynamic Scattering Experiments. In: Winter R (ed) *Advances in High*
604 *Pressure Bioscience and Biotechnology II*, Springer: Berlin, Heidelberg, pp 29–32.

605 Dubins, D.N., Lee, A., Macgregor, R.B., Chalikian, T.V. (2001). On the Stability of Double
606 Stranded Nucleic Acids. *Journal of the American Chemical Society* 123:9254–9259.

607 Eisenmenger, M.J., Reyes-De-Corcuera, J.I. (2009). High pressure enhancement of enzymes:
608 A review. *Enzyme and Microbial Technology* 45:331–347.

609 Erauso, G., Reysenbach, A.-L., Godfroy, A., Meunier, J.-R., Crump, B., Partensky, F., Baross,
610 J.A., Marteinsson, V., Barbier, G., Pace, N.R., Prieur, D. (1993). *Pyrococcus abyssi* sp. nov., a
611 new hyperthermophilic archaeon isolated from a deep-sea hydrothermal vent. *Arch*
612 *Microbiol* 160:338–349.

613 Girard, E., Prangé, T., Dhaussy, A.-C., Migianu-Griffoni, E., Lecouvey, M., Chervin, J.-C.,
614 Mezouar, M., Kahn, R., Fourme, R. (2007). Adaptation of the base-paired double-helix
615 molecular architecture to extreme pressure. *Nucleic Acids Res* 35:4800–4808.

616 Gouge, J., Ralec, C., Henneke, G., Delarue, M. (2012). Molecular Recognition of Canonical
617 and Deaminated Bases by *P. abyssi* Family B DNA Polymerase. *Journal of Molecular Biology*
618 423:315–336.

619 Gross, M., Jaenicke, R. (1994). Proteins under pressure. The influence of high hydrostatic
620 pressure on structure, function and assembly of proteins and protein complexes. *European*
621 *Journal of Biochemistry* 221:617–630.

622 Gross, M., Lehle, K., Jaenicke, R., Nierhaus, K.H. (1993). Pressure-induced dissociation of
623 ribosomes and elongation cycle intermediates. *European Journal of Biochemistry* 218:463–
624 468.

625 Gueguen, Y., Rolland, J., Lecompte, O., Azam, P., Romancer, G.L., Flament, D., Raffin, J.-P.,
626 Dietrich, J. (2001). Characterization of two DNA polymerases from the hyperthermophilic
627 euryarchaeon *Pyrococcus abyssi*. *European Journal of Biochemistry* 268:5961–5969.

628 Gunter, T.E., Gunter, K.K. (1972). Pressure dependence of the helix–coil transition
629 temperature for polynucleic acid helices. *Biopolymers* 11:667–678.

630 Hallsworth, J.E., Yakimov, M.M., Golyshin, P.N., Gillion, J.L.M., D’Auria, G., Alves, F.D.L., La
631 Cono, V., Genovese, M., McKew, B.A., Hayes, S.L., Harris, G., Giuliano, L., Timmis, K.N.,
632 McGenity, T.J. (2007). Limits of life in MgCl₂-containing environments: chaotropicity defines
633 the window. *Environmental Microbiology* 9:801–813.

634 Hedén, C.G., Lindahl, T., Toplin, I. (1964). The Stability of Deoxyribonucleic Acid Solutions
635 under High Pressure. *Acta Chemica Scandinavica* 18:1150–1156.

636 Henneke, G., Flament, D., Hübscher, U., Querellou, J., Raffin, J.-P. (2005). The
637 Hyperthermophilic Euryarchaeota *Pyrococcus abyssi* Likely Requires the Two DNA
638 Polymerases D and B for DNA Replication. *Journal of Molecular Biology* 350:53-64.

639 Henneke, G. (2012). In vitro reconstitution of RNA primer removal in Archaea reveals the
640 existence of two pathways. *Biochemical Journal* 447:271–280.

641 Heremans, K. (2009). Pressure Effects on Biomolecules. In: *Extremophiles - Volume III*,
642 *Encyclopedia of life support systems*. EOLSS Publications Vol III, p 9.

643 Hsu, H.-W., Postberg, F., Sekine, Y., Shibuya, T., Kempf, S., Horányi, M., Juhász, A., Altobelli,

644 N., Suzuki, K., Masaki, Y., Kuwatani, T., Tachibana, S., Sirono, S., Moragas-Klostermeyer, G.,
645 Srama, R. (2015). Ongoing hydrothermal activities within Enceladus. *Nature* 519:207–210.

646 Hughes, F., Steiner, R.F. (1966). Effects of pressure on the helix–coil transitions of the poly
647 A–poly U system. *Biopolymers* 4:1081–1090.

648 Jannasch, H.W., Wirsén, C.O., Molyneux, S.J., Langworthy, T.A. (1992). Comparative
649 Physiological Studies on Hyperthermophilic Archaea Isolated from Deep-Sea Hot Vents with
650 Emphasis on *Pyrococcus* Strain GB-D. *Appl Environ Microbiol* 58:3472–3481.

651 Jebbar, M., Franzetti, B., Girard, E., Oger, P. (2015). Microbial diversity and adaptation to
652 high hydrostatic pressure in deep-sea hydrothermal vents prokaryotes. *Extremophiles*
653 19:721–740.

654 Jebbar, M., Hickman-Lewis, K., Cavalazzi, B., Taubner, R.-S., Rittmann, S.K.-M.R., Antunes, A.
655 (2020). Microbial Diversity and Biosignatures: An Icy Moons Perspective. *Space Sci Rev*
656 216:10.

657 Kawano, H., Nakasone, K., Abe, F., Kato, C., Yoshida, Y., Usami, R., Horikoshi, K. (2005).
658 Protein–DNA Interactions under High-Pressure Conditions, Studied by Capillary Narrow-Tube
659 Electrophoresis. *Bioscience, Biotechnology, and Biochemistry* 69:1415–1417.

660 Kawano, H., Nakasone, K., Matsumoto, M., Yoshida, Y., Usami, R., Kato, C., Abe, F. (2004).
661 Differential pressure resistance in the activity of RNA polymerase isolated from *Shewanella*
662 *violacea* and *Escherichia coli*. *Extremophiles* 8:367–375.

663 Kong, H., Kucera, R.B., Jack, W.E. (1993). Characterization of a DNA polymerase from the
664 hyperthermophile archaea *Thermococcus litoralis*. Vent DNA polymerase, steady state
665 kinetics, thermal stability, processivity, strand displacement, and exonuclease activities. *J*
666 *Biol Chem* 268:1965–1975.

667 Lowell, R.P., DuBose, M. (2005). Hydrothermal systems on Europa. *Geophysical Research*
668 *Letters* 32.

669 Lundberg, K.S., Shoemaker, D.D., Adams, M.W.W., Short, J.M., Sorge, J.A., Mathur, E.J.
670 (1991). High-fidelity amplification using a thermostable DNA polymerase isolated from
671 *Pyrococcus furiosus*. *Gene* 108:1–6.

672 Macgregor, R.B. (1996). Chain length and oligonucleotide stability at high pressure.
673 *Biopolymers* 38:321–328.

674 Macgregor, R.B. (2002). The interactions of nucleic acids at elevated hydrostatic pressure.
675 *Biochimica et Biophysica Acta (BBA) - Protein Structure and Molecular Enzymology*
676 1595:266–276.

677 Marion, G.M., Fritsen, C.H., Eicken, H., Payne, M.C. (2003). The Search for Life on Europa:
678 Limiting Environmental Factors, Potential Habitats, and Earth Analogues. *Astrobiology*
679 3:785–811.

680 Matson, D.L., Castillo, J.C., Lunine, J., Johnson, T.V. (2007). Enceladus' plume: Compositional
681 evidence for a hot interior. *Icarus* 187:569–573.

682 Naganuma, T., Uematsu, H. (1998). Dive Europa: A Search-for-Life Initiative. *Biological*
683 *Sciences in Space* 12:126–130.

684 Pande, C., Wishnia, A. (1986). Pressure dependence of equilibria and kinetics of *Escherichia*
685 *coli* ribosomal subunit association. *Journal of Biological Chemistry* 261:6272–6278.

686 Pappalardo, R.T. (2012). *Europa Study 2012 Report*.

687 Pappalardo, R.T., Belton, M.J.S., Breneman, H.H., Carr, M.H., Chapman, C.R., Collins, G.C.,
688 Denk, T., Fagents, S., Geissler, P.E., Giese, B., Greeley, R., Greenberg, R., Head, J.W.,
689 Helfenstein, P., Hoppa, G., Kadel, S.D., Klaasen, K.P., Klemaszewski, J.E., Magee, K., McEwen,
690 A.S., Moore, J.M., Moore, W.B., Neukum, G., Phillips, C.B., Prockter, L.M., Schubert, G.,
691 Senske, D.A., Sullivan, R.J., Tufts, B.R., Turtle, E.P., Wagner, R., Williams, K.K. (1999). Does
692 Europa have a subsurface ocean? Evaluation of the geological evidence. *Journal of*
693 *Geophysical Research: Planets* 104:24015–24055.

694 Park, R.S., Bills, B., Buffington, B.B., Folkner, W.M., Konopliv, A.S., Martin-Mur, T.J.,
695 Mastrodemos, N., McElrath, T.P., Riedel, J.E., Watkins, M.M. (2015). Improved detection of
696 tides at Europa with radiometric and optical tracking during flybys. *Planetary and Space*
697 *Science* 112:10–14.

698 Nath, A., Subbiah, K. (2016). Insights into the molecular basis of piezophilic adaptation:
699 Extraction of piezophilic signatures. *Journal of Theoretical Biology* 390:117–126.

700 Ralec, C., Henry, E., Lemor, M., Killelea, T., Henneke, G. (2017). Calcium-driven DNA synthesis
701 by a high-fidelity DNA polymerase. *Nucleic Acids Res* 45:12425–12440.

702 Rayan, G., Macgregor, R.B. (2005). Comparison of the Heat- and Pressure-Induced Helix–Coil
703 Transition of Two DNA Copolymers. *The Journal of Physical Chemistry B* 109:15558–15565.

704 Rosenbaum, E., Gabel, F., Durá, M.A., Finet, S., Cléry-Barraud, C., Masson, P., Franzetti, B.
705 (2012). Effects of hydrostatic pressure on the quaternary structure and enzymatic activity of
706 a large peptidase complex from *Pyrococcus horikoshii*. *Archives of Biochemistry and*
707 *Biophysics* 517:104–110.

708 Schmidt, C., Manning, C.E. (2017). Pressure-induced ion pairing in MgSO₄ solutions:
709 Implications for the oceans of icy worlds. *Geochemical Perspectives Letters*:66–74.

710 Sekine, Y., Shibuya, T., Postberg, F., Hsu, H.-W., Suzuki, K., Masaki, Y., Kuwatani, T., Mori, M.,
711 Hong, P.K., Yoshizaki, M., Tachibana, S., Sirono, S. (2015). High-temperature water–rock
712 interactions and hydrothermal environments in the chondrite-like core of Enceladus. *Nature*
713 *Communications* 6:8604.

714 Spohn, T., Schubert, G. (2003). Oceans in the icy Galilean satellites of Jupiter? *Icarus*
715 161:456–467.

716 Summit, M., Scott, B., Nielson, K., Mathur, E., Baross, J. (1998). Pressure enhances thermal
717 stability of DNA polymerase from three thermophilic organisms. *Extremophiles* 2:339–345.

718 Taubner, R.-S., Olsson-francis, K., Vance, S., Ramkissoon, N., Postberg, F., de Vera, J.-P.,
719 Antunes, A., Camprubí Casas, E., Sekine, Y., Noack, L., Barge, L., Goodman, J., Jebbar, M.,
720 Journaux, B., Karatekin, Ö., Klenner, F., Rabbow, E., Rettberg, P., Rückriemen-Bez, T.,
721 Soderlund, K. (2020). Experimental and Simulation Efforts in the Astrobiological Exploration
722 of Exooceans. *Space Science Reviews* 216.

723 Taubner, R.-S., Pappenreiter, P., Zwicker, J., Smrzka, D., Pruckner, C., Kolar, P., Bernacchi, S.,
724 Seifert, A.H., Krajete, A., Bach, W., Peckmann, J., Paulik, C., Firneis, M.G., Schleper, C.,
725 Rittmann, S.K.-M.R. (2018). Biological methane production under putative Enceladus-like
726 conditions. *Nature Communications* 9:748.

727 Tehei, M., Zaccai, G. (2007). Adaptation to high temperatures through macromolecular
728 dynamics by neutron scattering. *The FEBS Journal*:4034–4043.

729 Thomas, P.C., Tajeddine, R., Tiscareno, M.S., Burns, J.A., Joseph, J., Lored, T.J., Helfenstein,
730 P., Porco, C. (2016). Enceladus's measured physical libration requires a global subsurface
731 ocean. *Icarus* 264:37–47.

732 Waite, J.H., Glein, C.R., Perryman, R.S., Teolis, B.D., Magee, B.A., Miller, G., Grimes, J., Perry,
733 M.E., Miller, K.E., Bouquet, A., Lunine, J.I., Brockwell, T., Bolton, S.J. (2017). Cassini finds
734 molecular hydrogen in the Enceladus plume: Evidence for hydrothermal processes. *Science*
735 356:155–159.

736 Zaccai, G. (2013). Ecology of Protein Dynamics. *Current Physical Chemistry* 3:9–16.

737 Zhang, L., Kang, M., Xu, J., Huang, Y. (2015). Archaeal DNA polymerases in biotechnology.
738 *Applied Microbiology and Biotechnology* 99:6585–6597.

739 Zolotov, M.Y. (2007). An oceanic composition on early and today's Enceladus. *Geophysical*
740 *Research Letters* 34.

741